



High-Performance Ga₂O₃ Diode Based on Tin Oxide Schottky Contact

DOI:
[10.1109/LED.2019.2893633](https://doi.org/10.1109/LED.2019.2893633)

Document Version
Accepted author manuscript

[Link to publication record in Manchester Research Explorer](#)

Citation for published version (APA):
Du, L., Xin, Q., Xu, M., Liu, Y., Mu, W., Yan, S., Wang, X., Xin, G., Jia, Z., Tao, X., & Song, A. (2019). High-Performance Ga₂O₃ Diode Based on Tin Oxide Schottky Contact. *IEEE Electron Device Letters*, 1-1. <https://doi.org/10.1109/LED.2019.2893633>

Published in:
IEEE Electron Device Letters

Citing this paper
Please note that where the full-text provided on Manchester Research Explorer is the Author Accepted Manuscript or Proof version this may differ from the final Published version. If citing, it is advised that you check and use the publisher's definitive version.

General rights
Copyright and moral rights for the publications made accessible in the Research Explorer are retained by the authors and/or other copyright owners and it is a condition of accessing publications that users recognise and abide by the legal requirements associated with these rights.

Takedown policy
If you believe that this document breaches copyright please refer to the University of Manchester's Takedown Procedures [<http://man.ac.uk/04Y6Bo>] or contact uml.scholarlycommunications@manchester.ac.uk providing relevant details, so we can investigate your claim.



High-Performance Ga₂O₃ Diode Based on Tin Oxide Schottky Contact

Lulu Du, Qian Xin, Mingsheng Xu, Yaxuan Liu, Wenxiang Mu, Shiqi Yan, Xinyu Wang, Gongming Xin, Zhitai Jia, Xu-Tang Tao, Aimin Song, *senior Member, IEEE*

Abstract—A high-performance Schottky diode based on a 600- μm -thick Cr-doped $\beta\text{-Ga}_2\text{O}_3$ single crystal has been fabricated using SnO_x as the Schottky contact. The SnO_x film was deposited in argon/oxygen mixture gas to ensure an oxygen-rich stoichiometry in Ga_2O_3 near the Schottky interface, thus reducing oxygen deficiency related interface state density. The SnO_x film included three components: Sn, SnO, and SnO_2 , as revealed by X-ray photoelectron spectroscopy characterization. The high quality Ga_2O_3 single crystal grown by an edge-defined film-fed method has a carrier concentration of $1.0 \times 10^{18} \text{ cm}^{-3}$ and an electron mobility of $\sim 90 \text{ cm}^2/\text{Vs}$. Current density-voltage characteristics of the Schottky diode demonstrated high performance with a large barrier height of 1.17 eV, a close-to-unity ideality factor of 1.02, and a high rectification ratio beyond 10^{10} . Frequency-dependent capacitance and conductance analysis revealed that the maximum active interface state density is 5.92×10^{13} at a frequency of 7 kHz.

Index Terms—Ga₂O₃, Schottky barrier diodes (SBDs), tin oxide (SnO_x).

I. INTRODUCTION

GALLIUM oxide, Ga₂O₃, has attracted extensive attention for the next generation power electronics and solar-blind optoelectronics due to its large breakdown electric field strength of 8 MV/cm and extremely wide bandgap of 4.5-4.9 eV [1]-[6]. Schottky contact quality is critical for Schottky diode power electronics, because it determines their key performances such as breakdown voltage, leakage current, and

rectification ratio, $I_{\text{on/off}}$ [7]-[13]. Recently, many efforts have been made to improve Ga₂O₃ Schottky contact quality [7]-[11]. Konishi et al. demonstrated that fluorine ion treatment can realize a barrier height, Φ_B , increase of 0.3 eV of Ga₂O₃ Schottky barrier diodes, SBDs [9]. Sasaki et al. developed MOS-type Ga₂O₃ SBDs with improved Φ_B of 1.07 eV but a slight deteriorated ideality factor, n [10]. Most of the reported Ga₂O₃ Schottky contacts used high work function metals such as Pt, Pd, Ni, and Au, for achieving large Φ_B [6], [7], [9], [10], [12], [13]. To the best of our knowledge, only Müller et al. demonstrated oxidized noble metal PtO_x as Ga₂O₃ Schottky contacts, and the diodes showed an extremely large Φ_B of 1.94 eV, an ideal n of 1.09, and a high $I_{\text{on/off}}$ of 4.5×10^9 at $\pm 2 \text{ V}$ [11]. For ZnO and InGaZnO SBDs, it has been demonstrated that a series of oxides such as AgO_x [14], PtO_x [15], PdO_x [16], and Ru-Si-O [17], [18], at Schottky interfaces can improve the Schottky contact quality due to reduction of oxygen deficiency related interface state density by ensuring oxygen-rich stoichiometry near the Schottky interface [14]-[18].

In contrast to the high work function metals such as Pt, Pd, Au, Ni, etc. which are usually expensive, Sn has a low work function and is inexpensive. In this work, we used reactively sputtered SnO_x as Schottky contacts to achieve high performance Ga₂O₃ SBD, providing a new effective way to fabricate high quality Schottky contact on Ga₂O₃.

II. EXPERIMENTAL DETAILS

Cr-doped $\beta\text{-Ga}_2\text{O}_3$ single crystal was grown by edge-defined film-fed growth method, and the (100)-oriented $\beta\text{-Ga}_2\text{O}_3$ plate with a thickness of $\sim 600 \mu\text{m}$ and a size of $2 \text{ mm} \times 10 \text{ mm}$ was obtained by cleaving the bulk single crystal. To form cathode ohmic contact, firstly, one surface of the cleaved Ga₂O₃ plate was etched with inductively coupled plasma (ICP) technique using a mixture gas of BCl₃ (15 sccm) and Ar (5 sccm) for 2 min under the ICP/RF power of 150 W/15 W and a chamber pressure of 10 mTorr. Then, Ti/Au (40 nm/20 nm) was deposited by e-beam evaporation onto the etched Ga₂O₃ plate surface, and a rapid thermal annealing in N₂ gas at 350 °C for 2 min was applied followed for improving the ohmic contact. A 200-nm-thick SnO_x layer was deposited by reactive sputtering using a pure Sn target (99.9%, 3 inch in diameter) at room temperature with a sputtering power of 50 W. The working pressure and oxygen partial pressure, P_{O} , during the sputtering were $\sim 5.7 \text{ mTorr}$ and 3.1%, respectively. Finally, the SnO_x film was capped with an e-beam evaporated Ti layer. The active area of the SBD is $7.1 \times 10^{-4} \text{ cm}^2$.

This work was supported by the National Key Research and Development Program of China (Grant No. 2016YFB0406502, 2016YFA0301200, and 2016YFA0201800), Engineering and Physical Sciences Research Council (EPSRC) (Grant No. EP/N021258/1), the Natural Science Foundation of China (61504044), the Natural Science Foundation of Shandong Province (ZR2018MF029 and ZR201709260014), the Key Research and Development Program of Shandong Province (2017GGX10111, 2017GGX10121 and 2018GGX101027), China Postdoctoral Science Foundation funded project (2016M590634), and the Fundamental Research Funds of Shandong University (2018JC037, 2018WLJH87, 2017TB0021, 2016WLJH44, and 2015WLJH36).

L. Du, Q. Xin, M. Xu, Y. Liu, S. Yan, and A. Song are with Center of Nanoelectronics, and School of Microelectronics, Shandong University, Jinan 250100, P. R. China (e-mail: xinq@sdu.edu.cn, mshxu@163.com).

L. Du, Q. Xin, M. Xu, Y. Liu, W. Mu, S. Yan, Z. Jia, X. Tao, and A. Song are with State Key Laboratory of Crystal Materials, Shandong University, Jinan 250100, P. R. China (e-mail: z.jia@sdu.edu.cn, txt@sdu.edu.cn).

X. Wang is with Institute of Thermal Science and Technology, Shandong University, Jinan 250061, P. R. China

G. Xin is with School of Energy and Power Engineering, Shandong University, Jinan 250061, P. R. China

A. Song is with School of Electrical and Electronic Engineering, University of Manchester, Manchester M13 9PL, United Kingdom.

The surface morphology and roughness of the Ga₂O₃ plate were analyzed by an atomic force microscope (AFM, Dimension FastScan™). The cross-sectional structure of Ti/SnO_x/Ga₂O₃ was analyzed using a scanning electron microscope (SEM, FEI Nova 450). The microstructure of the Ga₂O₃ plate was elucidated by a Raman spectrometer (Renishaw in Via-Reflex) using a 532-nm wavelength laser at a power of 5 mW. The chemical composition of the SnO_x film was characterized by X-ray photoelectron spectroscopy (XPS, ESCALAB 250Xi). The binding energy was calibrated by setting the C 1s signal at 284.6 eV. The current density-voltage, J - V , and capacitance-voltage, C - V , characteristics were measured using a semiconductor analyzer (Agilent 2902B) and an LCR meter (Agilent E4980A), respectively, at room temperature in dark.

III. RESULTS AND DISCUSSION

The Ga₂O₃ exhibits high transmittance and a clear absorption edge at ~ 260 nm, as shown in Fig. 1(a), corresponding to a band gap of ~ 4.8 eV. AFM analysis indicates that the cleaved Ga₂O₃ surface is atomically flat with a root mean square roughness of 0.3 nm in an area of $1 \times 1 \mu\text{m}^2$, as shown in the inset of Fig. 1(a). The Ga₂O₃ plate shows ten sharp and narrow Raman active peaks located at 113, 146, 171, 201, 346, 418, 477, 630, 659, and 768 cm⁻¹, as shown in Fig. 1(b), illustrating high crystallinity of the plate. The peak at 201 cm⁻¹ correlates to the characteristic vibration and translation mode of Ga-O chains [19]. The peaks between 300 and 500 cm⁻¹ relate to deformation of Ga₂O₆ octahedra [20], and the peaks between 600 and 800 cm⁻¹ attribute to the stretching and bending of GaO₄ tetrahedra [20].

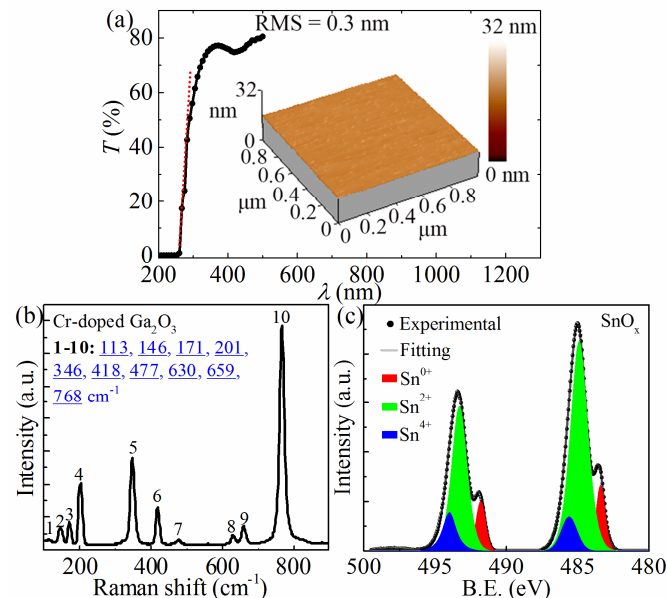


Fig. 1. Figure R1. UV-visible transmission spectrum (a) and Raman spectrum (b) of the Ga₂O₃ single crystal. (c) XPS of Sn 3d for the SnO_x film. Inset: AFM image of the Ga₂O₃ flake surface with root mean square surface roughness.

To determine the composition of the SnO_x film, an XPS measurement was carried, with the topmost native oxidized SnO₂ layer on the SnO_x film was sputtered away by low energy

(3 keV) argon plasma bombardments to get rid of its contribution. The XPS results illustrate that three compositions of Sn, SnO, and SnO₂ are included in the film, and the predominant composition is SnO. Figure 1(c) shows the Sn 3d_{5/2} and 3d_{3/2} spectra of with deconvoluted fittings (Gaussian + Lorentz (<30%)). The binding energy of the Sn 3d_{5/2} and 3d_{3/2} peaks centered at 484.4 and 492.8, 485.9 and 494.3, and 486.6 and 495.0 eV, corresponding to Sn⁰⁺, Sn²⁺, and Sn⁴⁺, respectively [21].

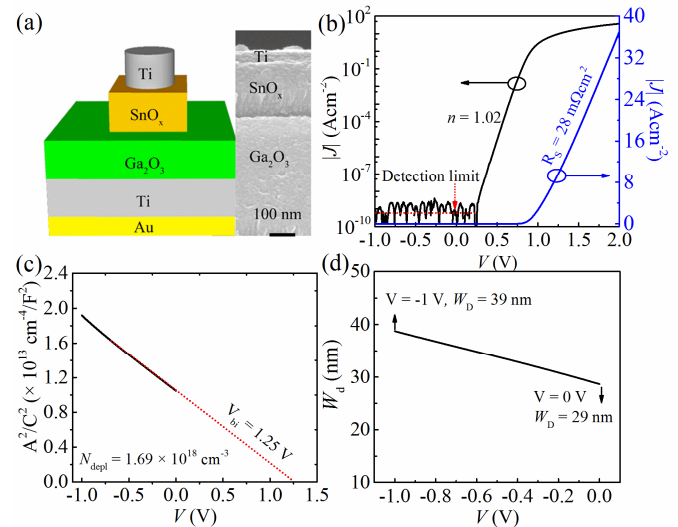


Fig. 2. (a) Schematic structure of the diode and SEM image of the cross-sectional structure of Ti/SnO_x/Ga₂O₃. (b) Semi-logarithmic and linear plots of a SnO_x/β-Ga₂O₃ SBD. A^2/C^2 (c) and width of the space charge region (d) in dependence on the applied voltage.

The morphology and electrical properties of the SnO_x/Ga₂O₃ SBD were investigated. Figure 2(a) shows the SEM image of the cross-sectional structure of Ti/SnO_x/Ga₂O₃, which shows two clear and smooth interfaces: SnO_x/Ga₂O₃ and Ti/SnO_x. Using the Richardson constant of 41.1 Acm⁻²K⁻² for β-Ga₂O₃ [3], [22], by fitting the forward J - V curve in Fig. 2(b) with the thermionic emission theory [23], the n and $\Phi_{B,JV}$ of the SBD are extracted as 1.02 and 1.17 eV, respectively. Here, the $\Phi_{B,JV}$ is defined as the Φ_B extracted by the J - V curve. The close-to-unity n indicates a very high quality Schottky interface between Ga₂O₃ and SnO_x. Such high performance is mainly due to that the main composition SnO in the SnO_x film usually contains a high density of tin vacancy defect states [24], [25]. Such tin vacancies induce oxygen dangling bonds which can compensate for oxygen vacancies in Ga₂O₃ at the Schottky interface. Thus, an insulating interfacial Ga₂O₃ layer with high oxygen stoichiometry at the SnO_x/Ga₂O₃ interface can be formed, leading to the large barrier height and near unity ideality factor. The ideality of the contact was further supported by the very low reverse current below our detection limit. The forward-bias current at $V > 0.9$ V is limited by the series resistance, R_s , of ~ 28 mΩ·cm² extracted from the slope of the J - V curve in linear scale in Fig. 2(b). The R_s of the SBD is larger than the resistance of the Ga₂O₃ layer, which is 4.2 mΩcm² given by $R = L/qn\mu_n$ [23]. Here, L is the thickness of the Ga₂O₃, μ_n is the mobility and is 90 cm²/Vs extracted by Hall effect measurement, and n is the carrier concentration and is $1.0 \times$

10^{18} cm^{-3} extracted by Hall effect measurement. The large R_s of SBD is contributed by the resistance of the insulating interfacial Ga_2O_3 layer. The SBD shows high performances such as a high $I_{\text{on/off}}$ of $> 10^{10}$, a large $\Phi_{\text{B},JV}$ of 1.17 eV, and a close-to-unity n of 1.02, which are comparable and even better than the reported high performance Ga_2O_3 SBDs with noble metal Schottky contacts [8], [10]-[12], [22], [26], [27].

To better understand the high quality Schottky contact interface, C - V measurement was performed and the results are plotted in Fig. 2(c) and (d). The built-in potential, V_{bi} , of 1.25 V and the background doping density in the depletion region, N_{depl} , of $1.69 \times 10^{18} \text{ cm}^{-3}$ were obtained by linear fitting of the C - V curve [23], as shown in Fig. 2(c) and Table I. This net donor concentration in the Ga_2O_3 extracted from the C - V characteristic is in reasonable agreement with the value of $1.0 \times 10^{18} \text{ cm}^{-3}$. The high doping limited the depletion region thickness to 29 nm at 0 V as shown in Fig. 2(d). The free charge density of the Ga_2O_3 layer estimated from the R_s value is $1.47 \times 10^{17} \text{ cm}^{-3}$ by using an electron mobility of $90 \text{ cm}^2/\text{Vs}$ [28]. The $\text{SnO}_x/\text{Ga}_2\text{O}_3$ SBD has a very low N_{depl}/N_c ratio of 11, indicating very low defect density, and this agrees well with the close-to-unity n of 1.02. The Schottky barrier extracted from the C - V characteristic, $\Phi_{\text{B},CV}$, is 1.34 eV by using $\Phi_{\text{B}} = qV_{\text{bi}} + kT/q \ln(N_c/N_e)$ [29], where the last term describing the energy gap between the conduction band and Fermi level is deduced to be 0.09 eV, and the conduction band density of states N_c is $5.2 \times 10^{18} \text{ cm}^{-3}$ [29]. A close agreement of $\Phi_{\text{B},JV}$ (1.17 eV) and $\Phi_{\text{B},CV}$ (1.34 eV) indicates that the $\text{SnO}_x/\text{Ga}_2\text{O}_3$ Schottky contact has relatively high uniformity.

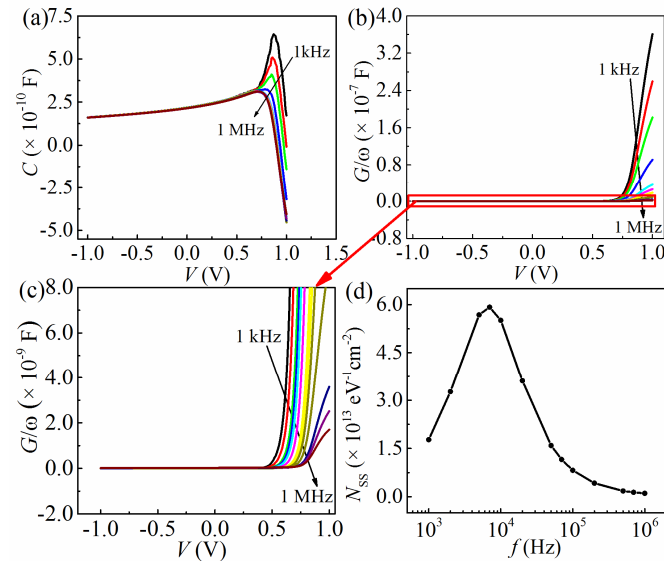


Fig. 3. Frequency dependence of (a) C - V and (b) G/ω - V characteristics of the $\text{SnO}_x/\beta\text{-Ga}_2\text{O}_3$ SBD. (c) Partially enlarged view of G/ω - V curve. (d) Variation of N_{ss} as a function of the frequency.

To evaluate the $\text{SnO}_x/\text{Ga}_2\text{O}_3$ interface state density, the dependences of C - V and conductance-voltage (G/ω - V) characteristics of the diode on the applied frequencies (1, 3, 5, 7, 10, 30, 50, 70, 100, 300, 500, 700, 1000 kHz) were investigated, as shown in Fig. 3(a) - (c). Here, $\omega = 2\pi f$ is the angular frequency, and G is the conductance. The value of C increased slightly with increasing applied bias voltage firstly due to the

decreasing depletion width, and then showed an anomalous peak at about 0.8 V due to the switching on of the diode, indicated also by Fig. 2(b) [30], [31]. This peak shows a decrease in value and a shift toward negative biases in position with increasing frequency. Such behavior is mainly due to the presence of interface states with various lifetimes [30], [31]. At low frequencies, the trap and de-trap of charges can follow the ac signal, and thus the charges at traps can contribute as excess capacitance to the measured capacitance (C_m). At high frequencies with voltage operation speed faster than the charge trap and de-trap speed, the charges at traps cannot contribute to the C_m any more. Figure 3(b) and (c) shows that under positive bias (~ 0.75 -1 V), the conductance increases slowly down with the increase of frequency, indicating the existence of interface states with different response time, and this is in good coordinate with the frequency dependent C .

Frequency dependence of interface state density, N_{ss} , distribution was obtained by using Hill-Coleman method [32]. According to this method, the value of N_{ss} can be determined from C and G/ω values for each frequency as following [32],

$$N_{\text{ss}} = \frac{2}{qA} \frac{(G/\omega)_m}{((G/\omega)_m/C_i)^2 + (I - C_m/C_i)^2} \quad (1)$$

here, $\omega = 2\pi f$ is the angular frequency, C_m is the peak value of the measured capacitance, and G is the conductance corresponding to C_m . C_i given by $C_i = C_m \left[1 + (G_m/\omega C_m)^2 \right]$ is the capacitance of the insulating interfacial Ga_2O_3 layer in strong accumulation at high frequency (1 MHz), and the value of C_i is 27 nF. The value of N_{ss} determined by Eq. (1) is shown in Fig. 3(d). The N_{ss} - f plot shows a peak and indicates that the activated N_{ss} reaches a maximum of 5.92×10^{13} at 7 kHz.

TABLE I
CHARACTERISTICS OF THE SBD FROM JV AND CV MEASUREMENTS

$\Phi_{\text{B},JV}$ (eV)	n	R_s ($\text{m}\Omega\text{cm}^2$)	$I_{\text{on/off}}$	N_c (cm^{-3})	qV_{bi} (eV)	N_{depl} (cm^{-3})	$\Phi_{\text{B},CV}$ (eV)
1.17	1.02	28	$> 10^{10}$	1.47×10^{17}	1.25	1.69×10^{18}	1.34

IV. CONCLUSION

In summary, a high performance $\beta\text{-Ga}_2\text{O}_3$ Schottky diode was fabricated using SnO_x as Schottky contact. The SnO_x film contains three components: Sn, SnO, and SnO_2 , of which SnO is the main component. The ultra-high quality Schottky contact interface was indicated by a near-unity ideality factor of 1.02, a large barrier height of 1.17 eV, and a high on/off ratio of $> 10^{10}$. This was achieved by that tin vacancies with oxygen dangling bonds in SnO compensate for oxygen vacancies in Ga_2O_3 at the Schottky interface and reduce the interface state density. The maximum active interface state density obtained by Hill-Coleman method is $5.92 \times 10^{13} \text{ eV}^{-1} \text{ cm}^{-2}$. The high-performance $\text{SnO}_x/\text{Ga}_2\text{O}_3$ diode shows that SnO_x film can be an excellent Schottky contact, which is inexpensive and convenient to deposit.

REFERENCES

- T. Onuma, S. Saito, K. Sasaki, T. Masui, T. Yamaguchi, T. Honda, M. Higashiwaki, "Valence band ordering in $\beta\text{-Ga}_2\text{O}_3$ studied by polarized transmittance and reflectance spectroscopy", *Japan. J. Appl. Phys.*, Vol. 54, No. 11, pp. 112601, Oct. 2015. DOI: [10.7567/JJAP.54.112601](https://doi.org/10.7567/JJAP.54.112601)

- [2] M. Higashiwaki, K. Sasaki, A. Kuramata, T. Masui, and S. Yamakoshi, "Gallium oxide (Ga_2O_3) metal-semiconductor field-effect transistors on single-crystal $\beta\text{-Ga}_2\text{O}_3$ (010) substrates", *Appl. Phys. Lett.*, Vol. 100, No. 1, pp. 013504, Jan. 2012. DOI: [10.1063/1.3674287](https://doi.org/10.1063/1.3674287)
- [3] H. He, R. Orlando, M. A. Blanco, R. Pandey, E. Amzallag, I. Baraille, M. Rerat, "First-principles study of the structural, electronic, and optical properties of Ga_2O_3 in its monoclinic and hexagonal phases", *Phys. Rev. B*, Vol. 74, No. 19, pp. 195123, Nov. 2006. DOI: [10.1103/PhysRevB.74.195123](https://doi.org/10.1103/PhysRevB.74.195123)
- [4] W. Y. Kong, G. A. Wu, K. Y. Wang, T. F. Zhang, Y. F. Zou, D. D. Wang, L. B. Luo, "Graphene- $\beta\text{-Ga}_2\text{O}_3$ Heterojunction for Highly Sensitive Deep UV Photodetector Application", *Adv. Mat.*, Vol. 28, No. 48, pp. 10725-10731, Oct. 2016. DOI: [10.1002/adma.201604049](https://doi.org/10.1002/adma.201604049)
- [5] T. P. Chow, I. Omura, M. Higashiwaki, H. Kawarada, V. Pala, "Smart Power Devices and ICs Using GaAs and Wide and Extreme Bandgap Semiconductors", *IEEE Trans. Electron Devices*, Vol. 64, No. 3, pp. 856-873, Feb. 2017. DOI: [10.1109/LED.2017.2653759](https://doi.org/10.1109/LED.2017.2653759)
- [6] Q. He, W. Mu, B. Fu, Z. Jia, S. Long, Z. Yu, Z. Yao, W. Wang, H. Dong, Y. Qin, G. Jian, H. Xue, H. Lv, Q. Liu, M. Tang, X. Tao, M. Liu, "Schottky Barrier Rectifier Based on (100) $\beta\text{-Ga}_2\text{O}_3$ and its DC and AC Characteristics", *IEEE Electron Device Lett.*, Vol. 39, No. 4, pp. 556-559, Mar. 2018. DOI: [10.1109/LED.2018.2810858](https://doi.org/10.1109/LED.2018.2810858)
- [7] Z. Hu, H. Zhou, Q. Feng, J. Zhang, C. Zhang, K. Dang, Y. Cai, Z. Feng, Y. Gao, X. Kang, Y. Hao, "Field-Plated Lateral $\beta\text{-Ga}_2\text{O}_3$ Schottky Barrier Diode with High Reverse Blocking Voltage of More Than 3 kV and High DC Power Figure-of-Merit of 500 MW/cm^2 ", *IEEE Electron Device Lett.*, Vol. 39, No. 10, pp. 1564-1567, Sep. 2018. DOI: [10.1109/LED.2018.2868444](https://doi.org/10.1109/LED.2018.2868444)
- [8] T. Watahiki, Y. Yuda, A. Furukawa, M. Yamamuka, Y. Takiguchi, S. Miyajima, "Heterojunction p-Cu₂O/n-Ga₂O₃ diode with high breakdown voltage", *Appl. Phys. Lett.*, Vol. 111, No. 22, pp. 222104, Nov. 2017. DOI: [10.1063/1.4998311](https://doi.org/10.1063/1.4998311)
- [9] K. Konishi, K. Goto, H. Murakami, Y. Kumagai, A. Kuramata, S. Yamakoshi, M. Higashiwaki, "1-kV vertical Ga_2O_3 field-plated Schottky barrier diodes", *Appl. Phys. Lett.*, Vol. 110, No. 10, pp. 103506, Mar. 2017. DOI: [10.1063/1.4977857](https://doi.org/10.1063/1.4977857)
- [10] K. Sasaki, D. Wakimoto, Q. T. Thieu, Y. Koishikawa, A. Kuramata, M. Higashiwaki, S. Yamakoshi, "First Demonstration of Ga_2O_3 Trench MOS-Type Schottky Barrier Diodes", *IEEE Electron Device Lett.*, Vol. 38, No. 6, pp. 783-785, Apr. 2017. DOI: [10.1109/LED.2017.2696986](https://doi.org/10.1109/LED.2017.2696986)
- [11] S. Müller, H. von Wenckstern, F. Schmidt, D. Splith, F. L. Schein, H. Frenzel, M. Grundmann, "Comparison of Schottky contacts on β -gallium oxide thin films and bulk crystals", *Appl. Phys. Express*, Vol. 8, No. 12, pp. 121102-1-121102-4, Nov. 2015. DOI: [10.7567/APEX.8.121102](https://doi.org/10.7567/APEX.8.121102)
- [12] J. Yang, S. Ahn, F. Ren, S. J. Pearton, S. Jang, J. Kim, A. Kuramata, "High reverse breakdown voltage Schottky rectifiers without edge termination on Ga_2O_3 ", *Appl. Phys. Lett.*, Vol. 110, No. 19, pp. 192101-1-192101-4, Apr. 2017. DOI: [10.1063/1.4983203](https://doi.org/10.1063/1.4983203)
- [13] Q. He, W. Mu, H. Dong, S. Long, Z. Jia, H. Lv, Q. Liu, M. Tang, X. Tao, M. Liu, "Schottky barrier diode based on $\beta\text{-Ga}_2\text{O}_3$ (100) single crystal substrate and its temperature-dependent electrical characteristics.", *Appl. Phys. Lett.*, Vol. 110, No. 9, pp. 093503, Mar. 2017. DOI: [10.1063/1.4977766](https://doi.org/10.1063/1.4977766)
- [14] M. W. Allen, S. M. Durbin, J. B. Metson, "Silver oxide Schottky contacts on n-type ZnO", *Appl. Phys. Lett.*, Vol. 91, No. 5, pp. 053512, Jul. 2007. DOI: [10.1063/1.2768028](https://doi.org/10.1063/1.2768028)
- [15] J. Zhang, Q. Xin, A. Song, "High performance Schotky diodes based on indium-gallium-zinc-oxide", *J. Vac. Sci. Technol. A*, Vol. 34, No. 4, pp. 04C101, Apr. 2016. DOI: [10.1116/1.4945102](https://doi.org/10.1116/1.4945102)
- [16] L. Du, J. Zhang, Y. Li, M. Xu, Q. Wang, A. Song, Q. Xin, "High-Performance Flexible Schottky Diodes Based on Sputtered InGaZnO", *IEEE Trans. Electron Devices*, Vol. 99, pp. 4326 - 4333, Oct. 2018. DOI: [10.1109/TED.2018.2864165](https://doi.org/10.1109/TED.2018.2864165)
- [17] J. Kaczmarek, M. A. Borysiewicz, K. Piskorski, M. Wzorek, M. Kozubal, E. Kamińska, "Flexible IGZO Schottky diodes on paper", *Semicond. Sci. Tech.*, Vol. 33, No. 1, pp. 015010, Nov. 2017. DOI: [10.1088/1361-6641/aa9acb](https://doi.org/10.1088/1361-6641/aa9acb)
- [18] J. Kaczmarek, J. Grochowski, E. Kamińska, A. Taube, M. A. Borysiewicz, K. Pągowska, W. Jung, A. Piotrowska, "Enhancement of Ru-Si-O/In-Ga-Zn-O MESFET performance by reducing depletion region trap density", *IEEE Electron Device Lett.*, Vol. 36, No. 5, pp. 469-471, Mar. 2015. DOI: [10.1109/LED.2015.2411749](https://doi.org/10.1109/LED.2015.2411749)
- [19] R. Rao, A. M. Rao, B. Xu, J. Dong, S. Sharma, M. K. Sunkara, "Blueshifted Raman scattering and its correlation with the [110] growth direction in gallium oxide nanowires", *J. Appl. Phys.*, Vol. 98, No. 9, pp. 094312, Nov. 2005. DOI: [10.1063/1.2128044](https://doi.org/10.1063/1.2128044)
- [20] S. Kumar, S. Dhara, R. Agarwal, R. Singh, "Study of photoconduction properties of CVD grown $\beta\text{-Ga}_2\text{O}_3$ nanowires", *J. Alloys Compounds*, Vol. 683, pp. 143-148, Oct. 2016. DOI: [10.1016/j.jallcom.2016.05.079](https://doi.org/10.1016/j.jallcom.2016.05.079)
- [21] H. Luo, L. Y. Liang, H. T. Cao, Z. M. Liu, F. Zhuge, "Structural, Chemical, Optical, and Electrical Evolution of SnO_x Films Deposited by Reactive rf Magnetron Sputtering", *ACS Appl. Mater. Inter.*, Vol. 4, No. 10, pp. 5673-5677, Oct. 2012. DOI: [10.1021/am301601s](https://doi.org/10.1021/am301601s)
- [22] K. Sasaki, M. Higashiwaki, A. Kuramata, T. Masui, S. Yamakoshi, "Schottky Barrier Diodes Fabricated by Using Single-Crystal $\beta\text{-Ga}_2\text{O}_3$ (010) Substrates", *IEEE Electron Device Lett.*, Vol. 34, No. 4, pp. 493-495, Mar. 2013. DOI: [10.1109/LED.2013.2244057](https://doi.org/10.1109/LED.2013.2244057)
- [23] S. M. Sze and K. K. Ng, *Physics of Semiconductor Devices*, 3rd ed. New York: Wiley, 2007.
- [24] Y. Li, Q. Xin, L. Du, Y. Qu, H. Li, X. Kong, Q. Wang, A. Song, "Extremely Sensitive Dependence of SnO_x Film Properties on Sputtering Power", *Sci. Rep.*, 6, 36183, Nov. 2016. DOI: [10.1038/srep36183](https://doi.org/10.1038/srep36183)
- [25] A. Togo, F. Oba, I. Tanaka, K. Tatsumi, "First-principles calculations of native defects in tin monoxide", *Phys. Rev. B: Condens. Mater.*, Vol. 74, No. 19, pp. 195128, Nov. 2006. DOI: [10.1103/PhysRevB.74.195128](https://doi.org/10.1103/PhysRevB.74.195128)
- [26] C. Joishi, S. Rafique, Z. Xia, L. Han, S. Krishnamoorthy, Y. Zhang, S. Lodha, H. Zhao, S. Rajan, "Low-pressure CVD-grown $\beta\text{-Ga}_2\text{O}_3$ bevel-field-plated Schottky barrier diodes", *Appl. Phys. Express*, Vol. 11, No. 3, pp. 031101, Feb. 2018. DOI: [10.7567/APEX.11.031101](https://doi.org/10.7567/APEX.11.031101)
- [27] A. Jayawardena, A. C. Ahyi, S. Dhar, "Analysis of temperature dependent forward characteristics of Ni/ $\beta\text{-Ga}_2\text{O}_3$ Schottky diodes", *Semicond. Sci. Tech.* Vol. 31, No. 11, pp. 115002, Sep. 2016. DOI: [10.1088/0268-1242/31/11/115002](https://doi.org/10.1088/0268-1242/31/11/115002)
- [28] Q. Xin, L. Yan, Y. Luo, A. Song, "Study of breakdown voltage of indium-gallium-zinc-oxide-based Schottky diode", *Appl. Phys. Lett.*, Vol. 106, No. 11, pp. 113506, Mar. 2015. DOI: [10.1063/1.4916030](https://doi.org/10.1063/1.4916030)
- [29] L. Du, H. Li, L. Yan, J. Zhang, Q. Xin, Q. Wang, A. Song, "Effects of substrate and anode metal annealing on InGaZnO Schottky diodes", *Appl. Phys. Lett.*, Vol. 110, No. 1, pp. 011602, Jan. 2017. DOI: [10.1063/1.4973693](https://doi.org/10.1063/1.4973693)
- [30] Ç. Bilkan, A. Gümüş, Ş. Altındal, "The source of negative capacitance and anomalous peak in the forward bias capacitance-voltage in Cr/p-si Schottky barrier diodes (SBDs)", *Mat. Sci. Semicon. Proc.*, Vol. 39, pp. 484-491, Nov. 2015. DOI: [10.1016/j.mssp.2015.05.044](https://doi.org/10.1016/j.mssp.2015.05.044)
- [31] Ş. Karataş, A. Türüt, "The determination of electronic and interface state density distributions of Au/n-type GaAs Schottky barrier diodes" *Physica B: Condens. Matter*, Vol. 381, No. 1-2, pp. 199-203, May. 2006. DOI: [10.1016/j.physb.2006.01.412](https://doi.org/10.1016/j.physb.2006.01.412)
- [32] W. A. Hill, C. C. Coleman, "A single-frequency approximation for interface-state density determination", *Solid State Electron.*, Vol. 23, No. 9, pp. 987-993, Sep. 1980. DOI: [10.1016/0038-1101\(80\)90064-7](https://doi.org/10.1016/0038-1101(80)90064-7)